Jordan Journal of Civil Engineering, Volume **16**, No. **4**, **2022**

Assessment of the Effects of Sinusoidal Steel Fibers and Polymer Fibers on Alkali-activated Concrete Pavement

Abolfazl Mohammadi Janaki [1)] ***and Gholam Ali Shafabakhsh*** [1)*]

[1)] Department of Civil Engineering, Semnan University, Semnan, Iran.
E-Mail: ghshafabakhsh@Semnan.ac.ir. * Corresponding Author.

ABSTRACT

The excessive use of cement has caused incremental production of greenhouse gases, one of the consequences of which is the overheating of the planet. These detrimental effects have highlighted the importance of pozzolanic materials and accordingly using alkali-activated concrete pavement instead of cement as a solution. Moreover, using fiber concrete surfaces is a predominant method to repair the concrete pavement due to the high speed of performance and the reduction of thickness. For this purpose, various amounts of sinusoidal steel fibers, kortta embass and kortta twist were added to alkali-activated concrete pavement. The results showed that with an increase in the fiber percentage, compressive strength, flexural strength, energy absorption, splitting tensile strength, impact resistance, skid resistance, resistance against freezing and thawing cycles are enhanced. On the other hand, the thickness of the concrete slab and water penetration into the concrete decreased. However, these cases are somewhat efficient for the sinusoidal steel fibers and then, the process begins to decrease.

KEYWORDS: Alkali-activated, Concrete pavement, Steel and polymer fibers, Mechanical features, Freezing and thawing durability.

INTRODUCTION

Pavements are divided into three general categories based on the type of material: flexible paving (asphalt), rigid paving (concrete) and composite paving. Flexible pavement has a surface covered with asphalt concrete. Rigid pavement is made of concrete, while composite pavement is a combination of both. Flexible pavement, also called asphalt pavement, is a structure that consists of several layers and its surface is covered with asphalt. In rigid pavement, the road surface is made of reinforced or unreinforced cement concrete, which is obtained by mixing Portland cement with sand and water. Composite pavement consists of an asphalt layer as a surface and a concrete layer under it (or *vice versa*) (Liu et al., 2020). The poor function of asphalt pavements in different weather conditions, rapid wearing of the surface, lack of proper durability and changes in the functional characteristics during the performance added to the uneconomical feature of this type of paving and lack of consistency with sustainable-development theories due to using oil-based pastes has pushed engineers and activists in this field to take more serious action than ever before to find concrete pavements suitable for various climatic situations (Horvath and Hendrickson, 1998; Jamshidi and White, 2019). On the other hand, easier access to materials, compatibility with the environment, lack of need for advanced technology and easier repair and maintenance of the concrete pavement have drawn attention to this pavement (Baloch et al., 2011; Shafabakhsh et al., 2020).

Moreover, since concrete is a brittle material, nowadays using fiber-reinforced concrete with higher softness that can bear changes in the form of the materials without breaking is carried out by researchers (Shen et al.). Fiber concrete is actually a type of composite that increases the tensile strength by using reinforcing fibers inside the concrete mix. The aims of using fibers in concrete pavement are increasing the

Received on 24/7/2021.
Accepted for Publication on 6/6/2022.

energy absorption of the concrete and controlling the spread of cracking so that the concrete piece can withstand the deformations on the cracked site against the imposed pressures after the initial crack. Reinforcing concrete with fibers is a technique which is generally based on randomly spreading the fibers on the concrete. Fiber application began in 1930 in developed countries and the material, shape and method of creation of reinforced concrete have changed a lot along with its applications over a period of four decades (Liew and Akhbar, 2020; Yang et al., 2018).

Alkali-activated concrete (AAC) can be more durable against freezing and thawing cycles considering the aluminum silicate (Si-O-Al) nature it possesses compared to cement concrete. Aluminum-silicate mineral polymer, which is also known as Alkali-activated concrete, has a three-dimensional structure, where geopolymer paste can serve instead of cement paste in concrete production (Rostami and Behfarnia, 2017; Awoyera and Adesina, 2020). In addition to lower durability and strength of cement concrete compared to alkali-activated concrete, concrete industry has faced challenges regarding CO_2 emissions, energy resources for production and alternative materials. On the other hand, taxes levied from the world organizations, named as green taxes, on cement production in factories with excessive pollutants have resulted in a rise in cement prices internationally (Shneider et al., 2020). The most common use for Portland cement is in the production of concrete, which has led to produce greenhouse gases, including CO_2 and global warming has been one of its consequences. More attention has been paid to alkali-activated concrete pavement as a solution because of these effects (Fu et al., 2011).

Davidovits reported that alkali-activated slag concrete produced from 80% to 95% less CO_2 emissions than conventional Portland cement (Davidovits, 2005).

Therfore, using alkali-activated concretes is a major and probably the most suitable mechanical method in enhancing expected features and minimizing weaknesses of a system (Mindess et al., 1981).

Ramli et al. used barchip fibers in high-strength concrete to provide local reinforcement effects to prevent cracks in the matrix. The results showed that 1.8% of barchip fibers can make the most progress in the concrete as the optimal percentage. When exposed on the long term, compressive strength was improved by more than 12% and permeability decreased (Ramli et al., 2013). Behfarnia and Behravan evaluated the performance of high-performance polypropylene fibers in concrete. The results showed that high-performance polypropylene fibers (such as barchip fibers) are not effective on steel fibers in terms of compressive strength, but have significant impacts on tensile strength, flexural strength, roughness and energy absorption (Behfarnia and Behravan, 2015). Yazici et al. investigated the effect of the amount of polyolefin fibers on the mechanical properties and then measured the impact resistance of roller-compacted concrete (RCC). The mechanical properties of RCC mixes including polyolefin were reduced by 20% compared to control mixtures without fibers. This phenomenon can be attributed to the increase in water-to-cement ratio of RCC mixtures in the presence of fibers (Yazici et al., 2013). Abdollahnejad et al. evaluated the effects of alkali-activated concrete with fly ash and polypropylene fibers and alcohol polyvinyl. The results proved that fly ash and fibers can reduce shrinkage and prolong its occurrence (Shah et al., 2020).

Manjunath et al. investigated alkali-activated concrete with self-compacting steel fibers. By increasing the steel fibers between 0.4% and 0.8% in alkali-activated concrete with high performance, compressive strength, flexural strength and toughness increased (Manjunath et al., 2020). Zhang et al. researched the self-healing features of alkali-activated concrete reinforced with polyvinyl alcohol fibers including crystal and bentonite mineral additives. X-rays revealed that healing mechanism generally occurs in superficial cracks and calcium carbonate was formed by the self-healing product. It was confirmed that by increasing pH and the concentration of calcium ions, along with using polyvinyl alcohol in the mixture to speed the process, the self-healing composites of alkali-activated concrete act synergistically (Zhang et al., 2020).

Zhou et al. studied the mechanical properties of alkali-activated concrete reinforced with basalt and polypropylene. They found that the length and the dose of PP fibers are not as efficient in improving the strength of alkali-activated concrete as basalts are (Zhou et al., 2020). Roesler et al. analyzed ultra-thin fiber concrete toppings and concluded that flexural strength, crack width control and increasing the load on the concrete topping are crucial factors in designing and choosing the

proper degree of fibers (Roesler et al., 2020).

Al-Taan and Al-Doski found that adding short discrete fibers to high-strength concrete (HSC) mixtures in reinforced concrete columns not only inhibits premature spalling of the concrete cover, but also enhances the strength of axially and eccentrically loaded reinforced columns (Al-Taan and Al-Doski, 2020). Also, Alabi found that 25% recycled concrete aggregate (RCA) with 1.5% lathe waste steel fiber (LWSF) improved compressive strength and workability, whereas split tensile strength substantially decreased (Alabi, 2020).

In recent years, to the best of our knowledge, little research has been focused on using alkali-activated concrete pavements. We aimed to evaluate the most common types of macro-fiber structures and their effects on alkali-activated concrete in terms of mechanical and functional properties. To investigate the influence of the fibers on the mechanical features and the durability of alkali-activated concrete, various percentages of sinusoidal steel fibers, kortta embass and kortta twist were used. Finally, compressive strength, flexural strength, energy absorption, splitting tensile strength, impact resistance, skid resistance, water penetration and resistance against freezing and thawing cycles were measured so that the best mixing plan is presented.

EXPERIMENTS

Materials

Like any other type of concrete, choosing the proper aggregate source is one of the most important factors of the quality and cost of the concrete. The used aggregates have a normal and natural weight. Grading used for making specimens is displayed in Table 1 according to ASTM C33 standard (Al-Taan and Al-Doski, 2020).

Table 1. Sieve aggregates' analysis

Coarse aggregates	Aggregate size (mm)	25	19	9.5	4.75	2.36
	Percentage of screening sieve (%)	100	96	38	8	0
Fine aggregates	Aggregate size (mm)	1.18	0.6	0.3	0.15	0.075
	Percentage of screening sieve (%)	82	58	26	7	2

Slag is the main binding material in the alkali-activated concrete composition. Slag was taken in ground form from Esfahan Steel Factory with a specific surface area of 3200 cm^2/g and a specific gravity of 2.754 g/cm^3 to make the samples. The chemical composition of the slag is shown in Table 2.

Table 2. Weights of chemical compounds in slag

Chemical composition	**Sio_2**	**CaO**	**Al_2O_3**	**MnO**	**SO_3**	**TiO_2**	**K_2O**	**MgO**	**P,Cl,Cr,Ni,Rb,Y,Th**
Slag	33.02	40.21	9.69	1.59	3.26	2.12	0.93	7.72	a few

In this study, three different types of fiber were used to evaluate the effects. These fiber types are sinusoidal steel fibers, kortta embass fibers and kortta twist fibers. Table 3 shows the characteristics of the used fibers.

Table 3. The characteristics of the used fibers

Fiber property	**Sinusoidal steel fibers**	**Kortta embass fibers**	**Kortta twist fibers**
Color	Metal gray	Light gray	Gray
Nominal length of fiber	50 mm	50 mm	50 mm
Nominal diameter of fiber	0.9 mm	0.5 mm	0.5 mm
Modulus of elasticity	200 GPa	6-7 GPa	5.5-6.5 GPa
Rupture strength	700-1200 MPa	550-700 MPa	600-700 MPa
Specific weight	7.85	0.91	0.92

Moreover, to activate the slag, a combination of sodium hydroxide (NaOH) and sodium silicate (Na_2SiO_3) is used.

Mixing Ratios

Mixing ratios used in this study were based on a volumetric method of ACI211-89 (ASTM, 2003). The samples are coded as AAS X I, standing for the active alkali slag concrete, X representing the type of the fiber and I is a two-digit number which shows the degree of fibers used in kilograms per cubic meter of concrete. For steel fibers which are used more in concrete (10 times more than polymer fibers), I directly indicate the weight of the fibers used in one cubic meter of concrete. Moreover, for other polymer fibers, I refer to the multiple of 10 by the weight of the fibers used in kilograms per cubic meter of concrete. In the mixing plan, activator was used so that Na_2O was 0.6 weight of the slag. Na_2O/SiO_2 ratio in all plans is considered to be one. Water was added to the degree that the ratio of water-to-cement materials became 0.425. The results of the mixing plan are presented in Table 4.

Table 4. The mixing ratios of alkali-activated concrete (kg/m^3)

Mix design	Coarse aggregates	Fine aggregates	Slag	Water	Sodium silicate	Sodium hydroxide	Fibers	
							Type of fibers	Mixing ratio
AAS	915	885	400	157.2	63	16.1	-	-
AASS10[1]	915	885	390	157.2	63	16.1	Sinusoidal steel	10
AASS15	915	885	385	157.2	63	16.1	Sinusoidal steel	15
AASS20	915	885	380	157.2	63	16.1	Sinusoidal steel	20
AASS25	915	885	375	157.2	63	16.1	Sinusoidal steel	25
AASE10[2]	915	885	399	157.2	63	16.1	Kortta Embass	1
AASE15	915	885	398.5	157.2	63	16.1	Kortta Embass	1.5
AASE20	915	885	398	157.2	63	16.1	Kortta Embass	2
AASE25	915	885	397.5	157.2	63	16.1	Kortta Embass	2.5
AAST10[3]	915	885	399	157.2	63	16.1	Kortta Twist	1
AAST15	915	885	398.5	157.2	63	16.1	Kortta Twist	1.5
AAST20	915	885	398	157.2	63	16.1	Kortta Twist	2
AAST25	915	885	397.5	157.2	63	16.1	Kortta Twist	2.5

[1] Akali-activated slag sinusoidal steel.

[2] Akali-activated slag kortta embass.

[3] Alkali-activated slag kortta twist.

Mix Design, Sampling and Curing Condition

To make concrete, an alkaline activator (sodium hydroxide and sodium silicate) was made the day before the test, because sodium hydroxide and water dissolve during the exothermic reaction. Next, all coarse aggregates were poured into a mixer with 50% activator and 50% slag and fibers and were mixed for thirty seconds. After that, all the remaining materials and the remaining 50% of the activator, slag and fibers were added and mixed for other 60 seconds. The curing of concrete samples in water is shown in Figure 1. The sample conditions are shown in Table 5.

Figure (1): The curing of concrete samples in water

Table 5. Lab program and sample conditions

Test	Sample dimensions	Age (days)	Number of samples in the mix	Curing conditions
Compressive strength	150 × 300 mm cylinder	28	3	Curing in water
Flexural strength and absorbing energy	500 × 100×100 mm	28	3	
Splitting tensile strength	150 × 300 mm cylinder	28	3	
Impact resistance	63.5 × 15 mm cylinder	28	3	
Slip resistance	-	28	3	
Depth of water permeability	200 × 200×120 mm	28	3	
Freezing and thawing cycles	370 × 78×78 mm	14,19,23,28,32, 37,41,46,50,54	3	

Test Procedures, Results and Discussion

Compressive Strength Test

Compressive strength is one of the most crucial parameters in evaluating the quality of concrete which is taken into consideration in pavements to determine durability and high compressive strength. The samples and machines used in this test were determined according to ASTM C39 (ACI, 1998).

As can be seen in Figure 2, in the mixing plan where steel fibers were added, with an increase in sinusoidal steel fibers, compressive strength increases. It is noteworthy that this increase has an optimum value which is 20 kg/m^3 and after that, there will be a decrease in compressive strength. In polymer fibers of kortta embass and kortta twist, the increase in fiber amount caused an increase in compressive strength. As expected from past experience, the addition of polymer fibers to concrete generally did not have a significant effect. However, steel fibers in amounts higher than a minimum will have a positive effect on this feature.

AASS20 has the highest compressive strength and its compressive strength increased compared to the control sample (AAS) by 27%. This sample can withstand more tension loads compared to other samples and the least compressive pressure is for the AAS sample. This issue can be because steel fibers have much more deformations (waves and screws) along their length and these properties cause the fibers to adhere better and engage with the concrete. Also, the compressive-strength results of all fiber-containing samples are higher than the compressive-strength results of those without fibers.

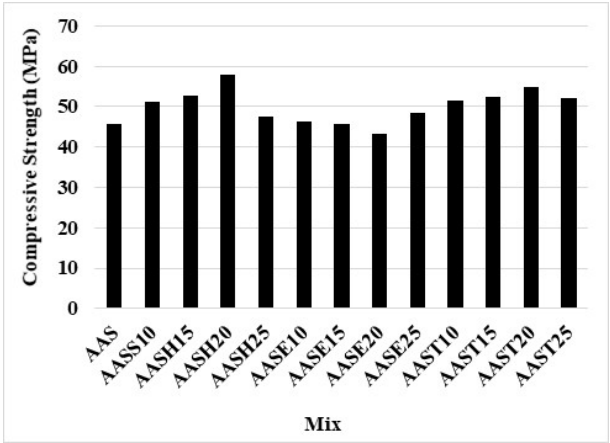

Figure (2): 28-day concrete compressive strength diagram

Flexural Strength and Energy Absorption Test

Flexural strength and rupture modulus are not only important factors of pavement, but also crucial elements in designing, being directly related to density and compressive strength, so that the density of the paste and the resistance of its binding with aggregate particles are high due to the ratio of cement to water and since the aggregates are compacted, minimizing the fatigue cracks. Rupture modulus is in accordance with ASTM C1609 based on pure bending and the degree of energy absorption of fiber-carrying concrete (ACI, 1998). As

depicted in Figure 3, the results from the bending test show that using fibers significantly increased compressive strength. We observed that AASS20 sample had the most positive reactions on this parameter, while the AASS20 sample had the highest bending strength (6.48MPa) and yet, it increased by 58% compared to the AAS samole. Steel fibers have a more effective role in improving the fracture modulus due to their modulus of elasticity and higher tensile stress. Accordingly, it is inferred that the main factors in increasing the fracture modulus of fiber concretes are tensile stress and high elastic modulus. The results show that when increasing the percentage of steel fibers in fiber-concrete samples, bending strength increases. The reason is that steel fibers can bridge the cracks once the first one is created because of their long lengths and thus, they prevent the growth of crack expansion. Accordingly, they can increase the flexural strength and ductility of concrete. Likewise, steel fibers bind better with the paste due to their shape (sinusoidal), which helps with a better performance after the first crack. In fact, uneven-shape and sinusoidal fibers have increased the extensional stress of steel fibers. The key points regarding the increase of bending strength of concrete mixtures reinforced with fibers are energy absorption and reduction of the width of cracks, which can influence the performance of concrete pavement.

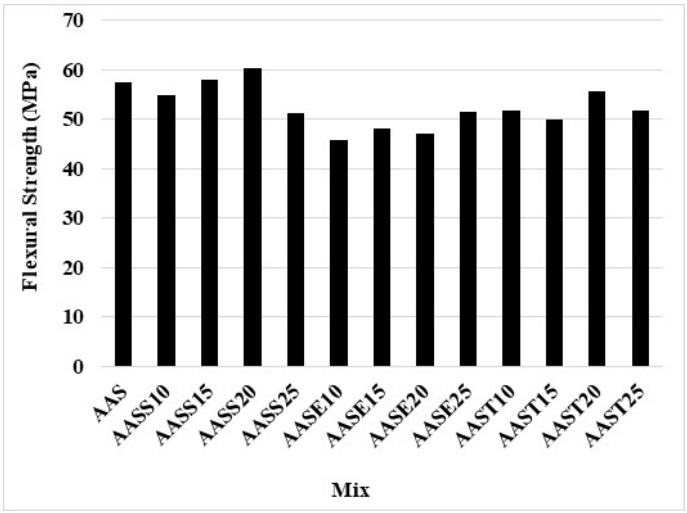

Figure (3): 28-day concrete flexural strength diagram

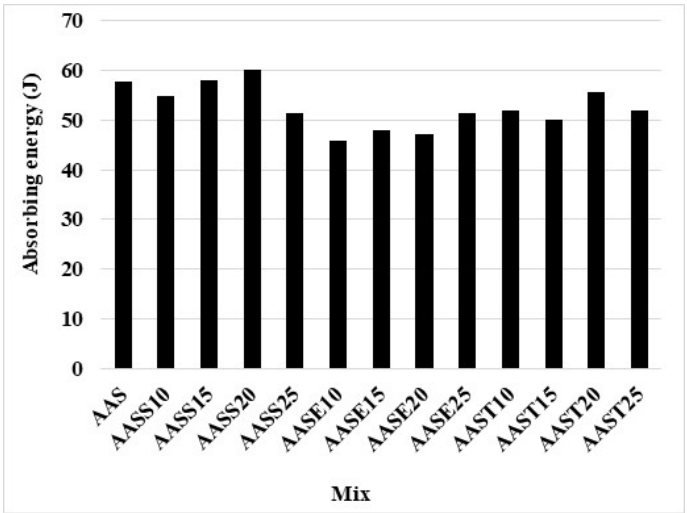

Figure (4): The energy absorption of concrete

Splitting Tensile Strength Test

Splitting tensile strength was imposed indirectly on the processed samples for 28 days in accordance with ASTM C496 (ASTM, 2012). As can be seen in Figure 5, significant influences are derived from steel and polymer fibers. The reason is that the fibers are spread homogeneously in all three dimensions of the structure of the concrete, therefore resulting in better load distribution, which by itself leads to an increase in splitting tensile strength. AASS20 had the most positive results in terms of this parameter; it has the highest splitting tensile strength (4.8MPa) and its splitting tensile strength has increased by 24% compared to AAS. The least splitting tensile strength belongs to AAS.

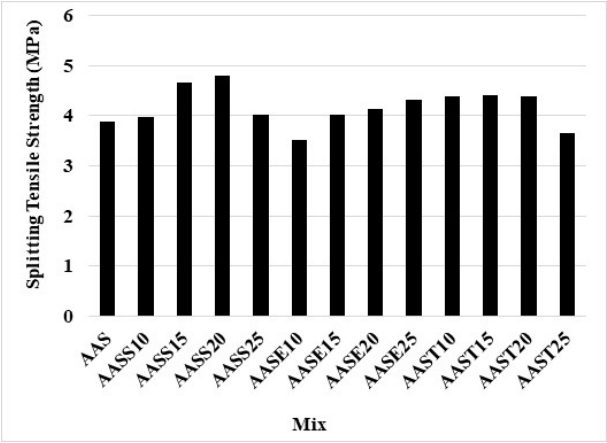

Figure (5): Comparison diagram of splitting tensile strengths

Impact Resistance

Impact resistance is tested according to one of the methods provided in ACI 544.2R regulations. In this study, we used the weight-drop method, which is the most proper one in testing fiber concrete (ASTM, 1996). According to Figure 6, it is apparent that the concrete models of AASE20 and AASS25 showed the most positive effects on the impact resistance of alkali-activated concrete, improving by 290% and 270%, respectively.

There are not many differences in the number of impacts required to create the first crack in the control samples and the fiber-concrete samples. In fact, the fibers play a more effective role after the first crack and the number of impacts required for the final failure of fiber-concrete samples is about 4 to 5.5 times that of the control sample. In fact, after the first crack is created, the fibers bridge the crack and prevent its spread, thus enhancing the impact resistance. The final failure method of fiber-concrete samples is different from that of concrete. At the final failure, the control specimens were broken into three separate pieces, while in the fiber-concrete specimens, the fibers maintained the cohesion of the specimens. In the samples, we observed that there is a difference in the number of impacts required to create the first fracture and the reason is the brittleness of the concrete. However, in fiber-concrete, the number of impacts required to break a piece of concrete is 4/5 times larger, the reason of which is that the fibers bridge the crack and prevent its spread. In the comparison of samples, fiber-concrete should be seen on the sample of steel-fiber concrete, where with increasing the percentage of steel fibers, the number of blows required for the final failure increases. Steel fibers are capable of bridging the large gaps (3cm) due to their lengths and can cause increases in splitting tensile strength and modulus of elasticity, thus increasing the impact resistance. On the other hand, the specific shape of steel fibers (wavy) makes them bind more with concrete, which increases the impact resistance even more.

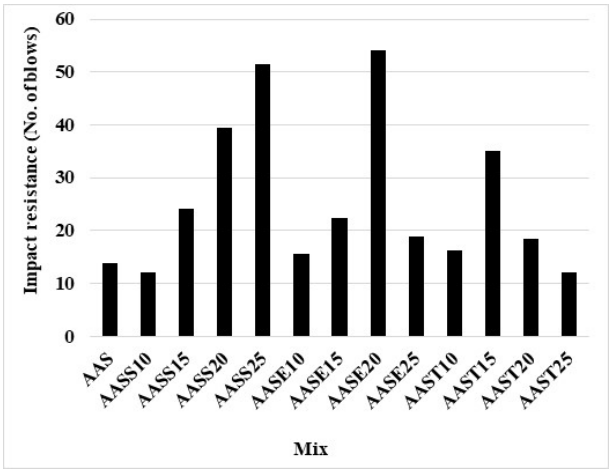

Figure (6): The results of impact resistance test

Skid Resistance Test

In this study, British pendulum tester was used to measure the skid resistance based on ASTM E303 guidelines (ACI, 1999). The skid resistance test had interesting results, which can be seen in Figure 7. Accordingly, all fibers with various degrees used in this tests, except for one, caused a negative influence in test results compared to control samples. AASS25 sample,

which had shown positive results in previous tests, could not improve the alkali-activated concrete. AASE25 sample was the most skid resistant (42.63BPN) and the least resistance belonged to AASS20 (35.63BPN).

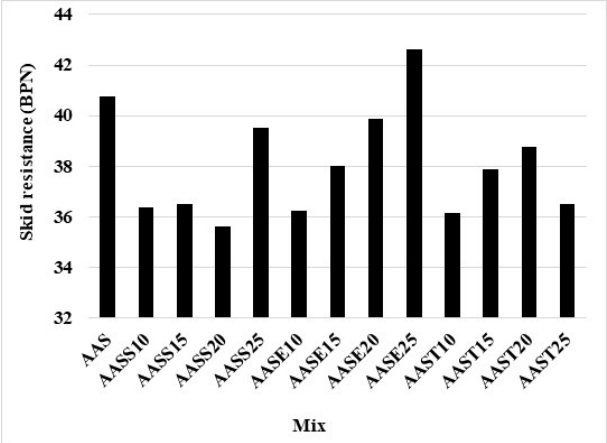

Figure (7): Skid resistance test results

Water Penetration Test in Concrete

To perform the test of water permeability under pressure, concrete samples sized 200×200×120 mm were created based on EN 12390-8 standard and after 28 days of processing, they were placed in a greenhouse at 100 degrees and were then put in 24 ±2 degrees to equate with room temperature. Next, the samples were placed under a penetration tester and a 5-bar pressure was imposed for 72 hours. Finally, the samples were split using Brazilian tester and the maximum depth of water penetration was measured (ASTM, 2018). Figure 8 depicts the changes of permeability regarding the fibers in alkali-activated concrete. Accordingly, at ratios of the mixtures in which the steel fibers replaced the slag, with increasing the sinusoidal steel fibers, the depth of concrete permeability reduces. It is noteworthy that this increase in the fibers has an optimal amount of about 20 kg/m^3 and after that, there will be an increase in the penetration of the depth of concrete. As experienced before, there was no significant influence on the concrete with adding polymer fibers. However, steel fibers left proper influences after a certain minimum. The least penetration depth of water in the sample was in AASS20 (17mm) and the most was in AAS (37mm). In AASS20 concrete sample, 54% progress was observed in reduced water permeability compared to AAS.

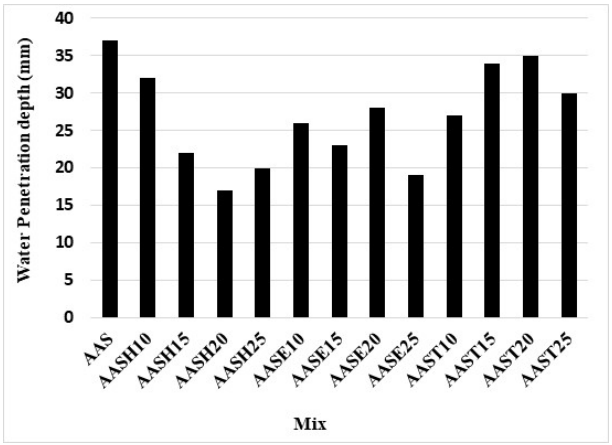

Figure (8): Water penetration depth in concrete

Freezing and Thawing Cycles

To evaluate the durability of concrete under freezing and thawing cycles, ultrasonic test was used in accordance with ASTM C666 standard. Samples were placed in freezing and thawing cycles after 14 days of processing. At a maximum of 36 cycles, the samples were taken out of the test, their pulse rate was read and the water was changed. This process was repeated until the samples went through 300 cycles and at the 300th cycle, their pulse rate was measured again (EN, 2009).

Ultrasonic pulse rate was measured according to ASTM C597 standard. Ultrasonic pulse velocity method involves measuring the velocity of pulses sent by the transmitter on one side of the concrete and received by the receiver on the other side of the concrete (ASTM, 2015). The results of ultrasonic test for concrete samples are shown in Table 6. The results clearly show the reduction of sample resistances when put in freezing and thawing cycles. The results show that at the 300th cycle, the highest pulse rate was related to AASS20 and the lowest was related to AAS. In fact, the most durable sample against freezing and thawing cycles was AASS20. By examining the ultrasonic pulse velocity, from the 180th cycle in most samples, the slope of the passing pulse velocity decreased and the pulse velocity decreased at a faster rate. From the 180th cycle to the 300th cycle, samples' pulse velocities either decreased or continued with the same values they had.

Table 6. Pulse transmission speed

Mix Design Name	Number of cycle									
	0	**36**	**72**	**108**	**144**	**180**	**216**	**252**	**288**	**300**
AAS	4570	4218	3851	3504	3161	2823	2461	2136	1778	1645
AASS10	4609	4221	3879	3519	3182	2837	2489	2144	1811	1684
AASS15	4732	4339	3967	3610	3262	2909	2553	2200	1858	1757
AASS20	4838	4436	4055	3691	3335	2974	2610	2249	1900	1776
AASS25	4815	4415	4036	3674	3319	2960	2598	2238	1891	1755
AASE10	4712	4321	3950	3595	3248	2896	2542	2190	1850	1752
AASE15	4723	4332	3961	3602	3257	2904	2550	2197	1854	1755
AASE20	4673	4278	3921	3565	3221	2862	2518	3162	1831	1739
AASE25	4830	4429	4049	3685	3330	2969	2606	2245	1897	1770
AAST10	4699	4309	3939	3585	3240	2888	2535	2184	1845	1750
AAST15	4601	4239	3875	3527	3187	2842	2494	2149	1815	1697
AAST20	4592	4230	3865	3525	3176	2840	2481	2158	1801	1668
AAST25	4614	4222	3859	3513	3174	2830	2484	2140	1808	1710

Concrete Pavement Slab Thickness

As can be seen from Figure 9, using fibers instead of slags reduced the thickness of the slab of the concrete pavement. At mixing ratios where steel fibers substituted slags, increasing the fibers reduced the thickness of the concrete slab. It is noteworthy that the increase in steel fibers has an optimal amount of about 20 kg/m^3 (AASS20) and then, the concrete slab becomes thick. In the polymer fibers of kortta embass and kortta twist, increasing the amount of fibers decreases the slab thickness. There was no a significant influence on the concrete with adding polymer fibers. But, steel fibers in amounts higher than a minimum will have a good positive effect on this property. The least slab thickness belonged to AASS20 (126mm) and the most belonged to AAS (158mm). In AASS20 concrete sample, 20.2% reduction of thickness was observed compared to AAS. In order to investigate the role of fibers in the design of concrete pavement slab thickness, the theory of yield lines was used and the results of this design method showed that the addition of fibers reduces the slab thickness by 22%.

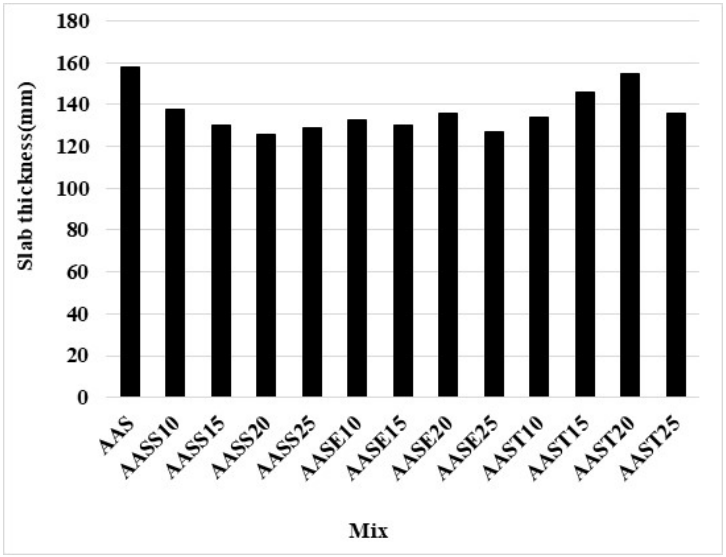

Figure (9): Thickness diagram of alkali-active slag concrete samples containing fibers

Relationship between Compressive-strength and Durability Tests

A linear relationship was written between the compressive-strength results and skid resistance, as well as between the flexural strength test and slab thickness (Figs. 10 and 11). There is a linear correlation with 0.601 between compressive strength and skid resistance, as seen in Fig. 10. There is a direct correlation with 0.992 regression coefficient between flexural strength and slab thickness, as seen in Fig. 11. This linear correlation shows that there is an inversely proportional relationship between compressive strength and skid resistance as well as between flexural strength and slab thickness. This means that, by increasing compressive strength and flexural strength, skid resistance and slab thickness are decreased, respectively.

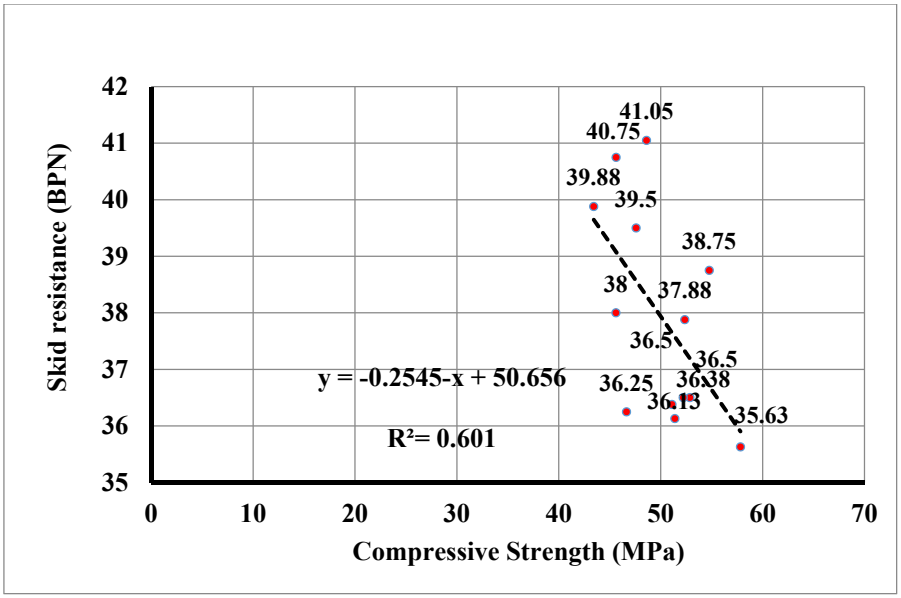

Figure (10): Relationship between compressive strength and skid resistance

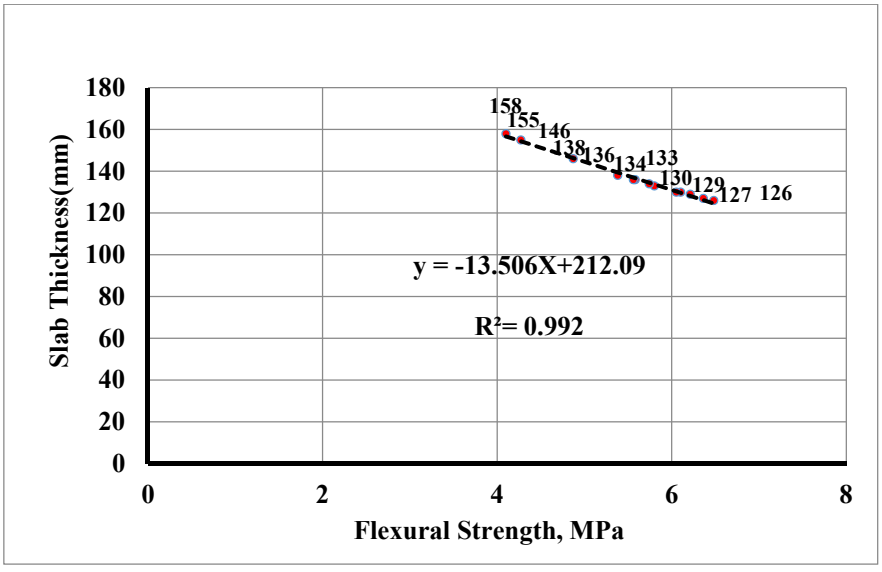

Figure (11): Relationship between flexural strength and slab thickness

CONCLUSIONS

The excessive use of cement has caused incremental production of greenhouse gases, one of the consequences of which is the overheating of the planet. These detrimental effects have highlighted the importance of pozzolanic materials and accordingly, using alkali-activated concrete pavement instead of cement has been presented as a solution. This study investigated the influences of fibers on the mechanical features and the durability of alkali-activated concrete, where various degrees of sinusoidal steel fibers, kortta embass fibers and kortta twist fibers were used to investigate their effects on compressive strength, flexural strength, energy absorption, splitting tensile strength, impact resistance, skid resistance, water penetration and resistance against freezing and thawing cycles.

1. By increasing the fiber percentage, compressive strength, splitting tensile strength, flexural strength, energy absorption, impact resistance, skid resistance and resistance against freezing and thawing cycles increased, while the thickness of the concrete slab and water penetration into the concrete decreased. However, these cases are somewhat efficient for sinusoidal steel fibers and then, the process begins to degenerate.
2. The highest compressive strength was observed in AASS20 compared to AAS. Moreover, the results of compressive strength of all fiber-including samples are higher than those of samples without fibers.
3. Using fibers significantly increased the compressive strength. AASS20 sample had the most positive reactions on this parameter.
4. AASS20 showed the most positive reactions on tensile resistance, where its resistance increased by 24% compared to AAS.
5. The concrete model of AASE20 and AASS25 showed the most positive effects on the impact resistance of alkali-activated concrete, improving by 290% and 270%, respectively.
6. AASS25 sample, which had shown positive results in previous tests, could not improve the alkali-activated concrete. AASE25 was the most skid-resistant sample.
7. The least penetration depth of water in the samples was in AASS20 (17mm) and the most was in AAS (37mm).
8. The highest pulse rate was related to AASS20 and the lowest was related to AAS. In fact, the most durable sample against freezing and thawing cycles was AASS20.
9. The least slab thickness belonged to AASS20 (126 mm) and the most belonged to in AAS (158mm). The addition of fibers reduced the slab thickness by 22%.

Acknowledgements

The authors would like to express their gratitude to Mr. Gharashi at the Laboratory of the Tarbiat Modares University for his helpful assistance.

Data Availability Statement

There is no data source for this research. All data is presented directly by graphs. All data, models and codes generated or used during the study appear in the submitted article.

REFERENCES

ACI 544.2R. (1999). “Measurement of properties of fiber-reinforced concrete”. American Concrete Institute, ACI Committee 544.

ACI Committee 211-89. (1998). “Standard practice for selecting proportions for normal, heavy-weight and mass concretes”. ACI Manual of Concrete Practice, Part 3.

Alabi, Stephen Adeyemi. (2020). “Predictive models for evaluation of compressive and split tensile strengths of recycled aggregate concrete containing lathe waste steel fiber”. Jordan Journal of Civil Engineering, 14 (4).

Al-Taan, Saad Ali, and Al-Doski, Abdul Jalil Sulaiman Ahmad. (2020). "Strength of steel fiber high-strength reinforced concrete columns under concentric and eccentric loads." Jordan Journal of Civil Engineering, 14 (4).

ASTM C1609/C1609M-12. (2012). "Standard test method for flexural performance of fiber-reinforced concrete (using beam with third-point loading)". ASTM International, West Conshohocken, PA.

ASTM C33. (2003). "Standard specification for concrete aggregates". American Standards for Testing and Materials, 04.02.

ASTM C39/C39M-18. (2018). "Standard test method for compressive strength of cylindrical concrete specimens". ASTM International, West Conshohocken, PA.

ASTM C496-96 (1996). "Standard test method for splitting tensile strength of cylindrical concrete specimens". ASTM International.

ASTM C597. (2015). "Standard test method for pulse velocity through concrete". ASTM International, West Conshohocken, PA.

ASTM C666. (2015). "Standard test method for resistance of concrete to rapid freezing and thawing". ASTM International, West Conshohocken, PA.

ASTM E303-93. (2018). "Standard test method for measuring surface frictional properties using the British pendulum tester". Vol. 93, Reapproved. ASTM International, West Conshohocken, PA, 1-5.

Awoyera, P., and Adesina, A. (2020). "Durability properties of alkali-activated slag composites: Short overview, J. Mag. Con. Res., 12 (16), 987-996.

Baloch, W.L., Khushnood, R.A., and Khaliq, W. (2011). "A review on the best practices in concrete-pavement design and materials in wet-freeze climates similar to Michigan". Transportation Research Record: J. Tra. Trans. Res. Bor., 6, 254-255.

Behfarnia, K., and Behravan, A. (2015). "Application of high-performance polypropylene fibers in concrete lining of water tunnels". J. Mat. Des., 55, 274-279.

Davidovits, J. (2005). "Geopolymer, green chemistry and sustainable-development solutions". Proceedings of The World Congress on Geopolymers, Geopolymer Institute.

EN 12390-3 (2009). "Standard testing of hardened concrete: Depth of penetration of water under pressure". European Committee for Standardization.

Fu, Y., Cai, L., and Wu, Y. (2011). "Freeze-thaw cycle test and damage-mechanics models of alkali-activated slag concrete". Constr. Build. Mater., 10 (1), 226.

Horvath, A., and Hendrickson, C. (1998). "Comparison of environmental implications of asphalt and steel-reinforced concrete pavements". J. Tra. Trans. Eng., 98 (661), 105-113.

Jamshidi, A., and White, G. (2019). "Evaluation of performance and challenges of use of waste materials in pavement construction: A critical review". J. Crit. Revi. Appl. Sci., 10 (1), 226.

Liew, K.M., and Akbar, A. (2020). "The recent progress of recycled steel fiber-reinforced concrete". Constr. Build. Mater., 232, 117232.

Liu, Y., Su, P., Li, M., You, Z., and Zhao, M. (2020). "Review on evolution and evaluation of asphalt-pavement structures and materials". Journal of Traffic and Transportation Engineering (English Edition), 7 (5), 573-599.

Manjunath, R., Narasimhan, M.C., and Kumar, S. (2020). "Effects of fiber addition on performance of high-performance alkali-activated slag concrete mixes: An experimental evaluation". Eur. J. Env. Civ. Eng., 78, 1-16.

Mindess, S., Young, J.F., and Darwin, D. (1981). "Concrete". Prentice-Hall Englewood Cliffs, NJ.

Ramli, M., Hoe Kwan, W., and Faisal Abas, N. (2013). "Application of non-corrosive barchip fibres for high-strength concrete enhancements in aggressive environments". J. Com.-Part B. Eng., 53, 134-144.

Roesler, J., Bordelon, A., Ioannides, A., Beyer, M., and Wang, D. (2008). "Design and concrete material requirements for ultra-thin whitetopping". Illinois Center for Transportaion, 1-181, 1-17.

Rostami, M., and Behfarnia, K. (2017). "The effect of silica fume on durability of alkali-activated slag concrete". Constr. Build. Mater., 134, 262-268.

Schneider, M., Romer, M., Tschudin, M., and Bolio, H. (2020). "Sustainable cement production: Present and future". Cem. Con. Res., 41 (7), 642-650.

Shafabakhsh, Gh., Mohammadi Janaki, A., and Jafari Ani, G. (2020). "Laboratory investigation on durability of nano-clay-modified concrete pavement". Eng. J., 24 (3), 35-44.

Shah, S.P., Konsta-Gdoutos, M.S., and Metaxa, Z.S. (2020). "High-strength fiber-reinforced one-part alkali-activated slag/fly ash binders with ceramic aggregates: Microscopic analysis, mechanical properties, drying shrinkage and freeze-thaw resistance". J. Mag. Con. Res., 241, 118129.

Shen, D., Wen, C., Zhu, P., Wu, Y., and Yuan, J. "Influence of barchip fiber on early-age autogenous shrinkage of high-strength concrete". Constr. Build. Mater., 256, 119223.

Yang, J.M., Shin, H.O., and Yoo, D.Y. (2018). "Benefits of using amorphous metallic fibers in concrete pavement for long-term performance". Arch. Civ. Mec. Eng., 17 (4), 750-760.

Yazici, A., Mardani, A., Tuyan, A., and Atacan Ute, M. (2013). "Mechanical properties and impact resistance of roller-compacted concrete containing polypropylene fibre". J. Mag. Con. Res., 67 (16), 867-875.

Zhang, L.V., Suleiman, A.R., and Nehdi, M.L. (2020). "Self-healing in fiber-reinforced alkali-activated slag composites incorporating different additives". Constr. Build. Mater., 262, 120059.

Zhou, X., Zeng, Y., Chen, P., Jiao, Z., and Zheng, W. (2020). "Mechanical properties of basalt and polypropylene fibre-reinforced alkali-activated slag concrete". Constr. Build. Mater., 121284.